

# Would you like to accelerate your time to results?

Find a manufacturing partner who can meet your current and future needs.



Let's **TALK**  
**CUSTOM**



Custom manufacturing often appears daunting, with so many options, standards and possibilities. There's no need to figure it out alone. We will help you find the right solution for your specifications and your timetable.



Learn more with our free webinar:  
[promega.com/CustomWebinar](https://promega.com/CustomWebinar)



# Bone morphogenetic protein signaling regulates Id1-mediated neural stem cell quiescence in the adult zebrafish brain via a phylogenetically conserved enhancer module

Gaoqun Zhang<sup>1</sup> | Marco Ferg<sup>1</sup> | Luisa Lübke<sup>1</sup> | Masanari Takamiya<sup>1</sup> |  
Tanja Beil<sup>1</sup> | Victor Gourain<sup>1</sup> | Nicolas Diotel<sup>2</sup> | Uwe Strähle<sup>1</sup> | Sepand Rastegar<sup>1</sup>

<sup>1</sup>Institute of Biological and Chemical Systems-Biological Information Processing (IBCS-BIP), Karlsruhe Institute of Technology (KIT), Karlsruhe, Germany

<sup>2</sup>Université de La Réunion, INSERM, UMR 1188, Diabète athérothrombose Thérapies Réunion Océan Indien (DÉTRO), Saint-Denis de La Réunion, France

## Correspondence

Uwe Strähle, PhD, and Sepand Rastegar, PhD, Institute of Biological and Chemical Systems-Biological Information Processing (IBCS-BIP), Karlsruhe Institute of Technology (KIT), Postfach 3640, 76021 Karlsruhe, Germany. Email: uwe.straehle@kit.edu (U. S.) and sepand.rastegar@kit.edu (S. R.)

## Funding information

FP7 Health, Grant/Award Number: FP7-242048; the European Union's Horizon 3952020 research and innovation programme under the Marie Skłodowska-Curie grant agreement, Grant/Award Number: ZENCODE-ITN 643062; European Union

## Abstract

In the telencephalon of adult zebrafish, the *inhibitor of DNA binding 1 (id1)* gene is expressed in radial glial cells (RGCs), behaving as neural stem cells (NSCs), during constitutive and regenerative neurogenesis. Id1 controls the balance between resting and proliferating states of RGCs by promoting quiescence. Here, we identified a phylogenetically conserved cis-regulatory module (CRM) mediating the specific expression of *id1* in RGCs. Systematic deletion mapping and mutation of conserved transcription factor binding sites in stable transgenic zebrafish lines reveal that this CRM operates via conserved *smad1/5* and *4* binding motifs under both homeostatic and regenerative conditions. Transcriptome analysis of injured and uninjured telencephala as well as pharmacological inhibition experiments identify a crucial role of bone morphogenetic protein (BMP) signaling for the function of the CRM. Our data highlight that BMP signals control *id1* expression and thus NSC proliferation during constitutive and induced neurogenesis.

## KEYWORDS

adult neurogenesis, BMP, cis-regulatory modules, *id1*, neural stem cell, radial glial cell, regeneration, telencephalon, transcription, zebrafish

## 1 | INTRODUCTION

In contrast to the mammalian adult brain, which contains only two main neurogenic regions that are both located in the forebrain and have rather limited ability to generate new neurons or to repair an injury, the brain of adult zebrafish contains numerous proliferative regions.<sup>1-3</sup> These are distributed throughout different subdivisions of

the brain and show high reactivation and repair capability upon lesion during adulthood.<sup>4-7</sup>

The ventricular zone of the adult zebrafish telencephalon is the most extensively studied neurogenic region in this context. This region produces new neurons, which integrate into existing neural networks throughout the lifetime of the animal.<sup>1,2,8,9</sup> It is densely populated by the cell bodies of radial glia cells (RGCs), which are the neural stem cells (NSCs) of the adult telencephalon.<sup>9,10</sup> The cell bodies of the RGCs extend two processes: a short one to the ventricular surface and a long one that crosses the brain parenchyma to reach the pial

Gaoqun Zhang and Marco Ferg contributed equally to this study.

This is an open access article under the terms of the Creative Commons Attribution-NonCommercial-NoDerivs License, which permits use and distribution in any medium, provided the original work is properly cited, the use is non-commercial and no modifications or adaptations are made.

©2020 The Authors. STEM CELLS published by Wiley Periodicals, Inc. on behalf of AlphaMed Press 2020

surface.<sup>9,11</sup> Under homeostatic conditions, the majority of RGCs are quiescent (type 1)<sup>9,12,13</sup> and express typical neural stem cell markers such as glial acidic fibrillary protein (Gfap), brain lipid binding protein (Blbp), and the calcium-binding protein  $\beta$  (S100 $\beta$ ).<sup>9,10,14</sup> Only a very low percentage of RGCs proliferate (type 2) and express the proliferative cell nuclear antigen (PCNA). This latter population can give rise to new neuroblasts (type 3 cells), either through asymmetric division or through direct conversion.<sup>15</sup>

A stab wound injury inflicted upon the telencephalon of adult zebrafish leads to an increase in NSC proliferation from 48 hours to 13 days postinjury<sup>16</sup> and a concomitant sustained production of new neurons that migrate from the ventricular layer to the injury site to replace the damaged/lost neurons.<sup>17-20</sup> Remarkably, 3 weeks after the brain injury, the fish feed and breed normally, barely exhibiting histological traces of the traumatic damage.<sup>17-21</sup> To quickly and efficiently replace dying/dead neurons, the number of RGCs entering the cell cycle and starting proliferation is greatly increased during regenerative neurogenesis.<sup>15,17,19,20</sup> Inflammatory signaling molecules cause expression of Gata3, a zinc finger transcription factor necessary for proliferation of RGCs, neurogenesis and migration of newborn neuroblasts.<sup>5,22</sup> In order to maintain a continuous supply of new neurons and to simultaneously prevent the exhaustion of the adult NSC pool, a tight control between quiescence, proliferation, differentiation, and self-renewal of the RGCs is crucial. In a screen for transcriptional regulators expressed in the telencephalon of adult zebrafish, we previously identified the *helix-loop-helix factor id1* (inhibitor of DNA binding 1) as a key player of both homeostatic and regenerative neurogenesis.<sup>23-25</sup> *id1* is mostly expressed in quiescent RGCs, and its expression is upregulated in the ventricular zone upon telencephalic injury. Forced expression of *id1* causes quiescence of NSCs, while *id1* knockdown increases the number of proliferating RGCs.<sup>25</sup> *id1* reduces cycling NSCs both during constitutive neurogenesis and after the initial wave of induction of proliferation in reactive neurogenesis.<sup>25</sup> Our data argue for a role of *id1* in maintaining the balance between dividing and resting NSCs by promoting RGC quiescence. We speculated that this might prevent depletion of the NSC pool.

Neither Notch signaling nor inflammatory signals appear to be involved in regulating *id1* expression in the adult telencephalon.<sup>25</sup> These data raised the central question of how and by which specific signals *id1* expression is restricted to adult neural stem cells and is upregulated after brain injury. To address these questions, we decided to investigate the mechanisms of transcriptional regulation of this gene during constitutive and regenerative neurogenesis.

We identified a phylogenetically conserved *id1* cis-regulatory module (CRM) that drives GFP expression in RGCs of the adult brain of transgenic zebrafish. This RGC-specific CRM harbors transcription factor (TF) binding sites conserved between human, mouse, and zebrafish *id1* homologues. Deletion mapping, mutations of the binding sites, as well as pharmacological inhibition and transcriptome analysis suggest a role for the BMP pathway in controlling *id1* expression in RGCs both during constitutive and regenerative neurogenesis.

### Significance statement

In the adult brain, to maintain a continuous supply of new neurons and to avoid the exhaustion of the neural stem cells (NSCs) pool, a tight control between quiescence and proliferation is crucial. The *inhibitor of DNA binding 1* (*id1*) gene controls the balance between dividing and resting neural stem cells by promoting quiescence. A regulatory sequence of *id1* was identified, which mediates the input from the bone morphogenetic protein signaling into the adult NSCs. This regulatory sequence has a high potential to serve as an interface, which will permit to alter the balance between proliferation and maintenance of stem cells in experimental, as well as medical, applications.

## 2 | MATERIALS AND METHODS

### 2.1 | Zebrafish strains and maintenance

All experiments were performed on 6- to 12-month-old AB wild-type (wt) fish or on the transgenic reporter line described in this article. Zebrafish housing and husbandry were performed as recommended by Reference 26. Animal experimentations were carried out in accordance with the German animal protection standards and were approved by the Government of Baden-Württemberg, Regierungspräsidium Karlsruhe, Germany (Aktenzeichen 35-9185.81/G-272/12 and 35-9185.81/G-288/18 "Adulte Neurogenese").

### 2.2 | Identification and cloning of putative CRMs

Identification of CRMs driving *id1* expression in zebrafish was based on their conservation in comparison to other fish species. We utilized Ancora (<http://ancora.genereg.net>) to select sequences for functional analysis. Ancora represents a database of highly conserved noncoding elements (HCNEs) that are identified by scanning pairwise BLASTZ net whole-genome alignments with different similarity parameters.<sup>27</sup> Criteria to be selected for functional testing were 80% sequence identity in a 50 bp window in all of the species *Oryzias latipes*, *Gasterosteus aculeatus*, and *Tetraodon nigroviridis* within a 100 kb window around the *id1* locus. Genomic coordinates in putative CRMs chosen to test for regulatory potential were polymerase chain reaction (PCR)-amplified from genomic DNA. Amplicons were subcloned into pCR8/GW/TOPO (Invitrogen) to create entry vectors for subsequent cloning into the Tol2-GFP-destination vector pT2KHGpzGATA2C1 as described by.<sup>28</sup> These constructs were used to generate stable zebrafish transgenic lines. The sequences of all CRMs are provided in Appendix S1.

### 2.3 | Mutation and deletion of different binding sites in the *id1* core sequence

Individual TF binding sites were mutated by converting the core sequence of the binding site as defined by MatInspector to a stretch of thymidines. The approach was PCR-based by employing primers designed to include the desired change.

Deletions were created using a similar methodology, a PCR-based approach using tailed primers designed to overlap with and anneal to the opposite strand of the adjoining region. The sequences of all primers used in this study can be found in Appendix S2.

### 2.4 | Injection of plasmids

For the generation of transgenic fish via a Tol2-based approach,<sup>29</sup> 50 ng/ $\mu$ L plasmid DNA was injected. The injection solution was prepared by adding 1% of phenol red and 30 ng/ $\mu$ L Tol2 mRNA. After injection the embryos were incubated at 28°C until they reached the desired stage. Embryos expressing GFP at 24 hpf were selected and the expression patterns documented. Identified F0 were out-crossed with wt fish to obtain stable progenies that express the transgene in the F1 generation. Each reporter construct was tested in at least three independent transgenic lines.

### 2.5 | Stab wound and chemical treatment of adult zebrafish

The stab wound injury was always inflicted in the left telencephalic hemisphere while the contralateral right hemisphere was kept intact and served as a control. Three to seven animals per transgenic line were tested for GFP induction upon telencephalon injury.

The stab wound procedure was performed as described.<sup>21</sup> For the treatment, 9-month-old *Tg(id1-CRM2:GFP)* fish were bathed in 300 mL fresh fish water containing 600  $\mu$ L of a 10 mM DMH1 (Tocris, Wiesbaden-Nordenstadt, Germany) stock solution (final concentration 20  $\mu$ M) for 7 days. As a control, 600  $\mu$ L of DMSO were added to 300 mL of fresh fish water. Every morning the fish were fed with regular adult fish food and the DMH1 or DMSO solution was changed every 2 days. Stab wounds were inflicted as described on the second day of treatment and the fish sacrificed for analysis 5 days after the injury. All experiments were carried out independently at least three times.

### 2.6 | Preparation of adult zebrafish brains, in situ hybridization, immunohistochemistry, imaging, and quantification

Brain dissection, in situ hybridization, and immunohistochemistry were performed as described in References 1 and 21. Primary antibodies used in this study include chicken anti-GFP (1:1000, Aves

labs, Davis, California), mouse anti-PCNA (1:500, Dako, Agilent, Santa Clara, California) and rabbit anti-S100 (1:400, Dako). Secondary antibodies were conjugated with Alexa fluor dyes (Alexa series) and include anti-GFP Alexa 488, antimouse Alexa 546 and anti-rabbit Alexa 633 (1:1000, Invitrogen, Waltham, Massachusetts). Pictures of in situ hybridized sections were acquired with a Leica compound microscope (DM5000B). For imaging and quantification immunohistochemistry brain slices mounted in Aqua-Poly/Mount (Cat No. 18606-20, Polysciences, Inc) with #1.5 thickness coverslips were imaged with a laser scanning confocal microscope Leica TCS SP5. To obtain single-cell resolution images, an HCX PL APO CS x63/1.2NA objective was used with the pinhole size set to 1-airy unit. Fluorescent images for GFP, PCNA, and S100 $\beta$  were acquired sequentially in 16-bit color depth with excitation/emission wavelength combinations of 488 nm/492 to 550 nm, 561 nm/565 to 605 nm, and 633 nm/650 to 740 nm, respectively. Pixel resolution for XY and Z planes are 0.24 and 0.50  $\mu$ m, respectively. For individual brain samples, at least three transverse sections cut with a vibratome (VT1000S, Leica) at different anterior-posterior levels representing anterior, posterior and intermediate telencephalic regions were imaged.

In order to quantify the changes in *bambina*, *id3*, and *smad5* mRNAs following brain injury at 5 days postlesion, up to 11 telencephalic pictures at the injury site were taken for each of the genes. Then, using ImageJ, the pictures were processed setting up a threshold for the staining intensity and quantification of the upregulated area was performed along the control and stab-wounded ventricular zone from the dorsomedial to the dorsolateral part of the telencephalon. The fold induction between the injured vs control ventricular zone was subsequently calculated.

### 2.7 | Image analysis

Confocal brain images were opened with Fiji/ImageJ software<sup>30</sup> as composite hyperstacks to manually evaluate colocalization of GFP, PCNA, and S100 $\beta$  proteins. Colocalization of fluorescent signals was assessed by at least two experimenters. For quantifications, three sections per brain were analyzed. Cells were counted in the dorsomedial and the dorsolateral ventricular zone.

### 2.8 | Statistical analysis

For quantifications of *id1-CRM2:GFP* and derivative constructs, the number of cells was determined by counting the cells in Z-stacks of 50  $\mu$ m thickness in 1  $\mu$ m steps ( $\times$ 40 objective lens). Comparisons between two data sets and between more than two data sets were performed using Welch two sample t-test and one-way ANOVA followed by Tukey's multiple pairwise-comparison test, respectively. Statistical significance was assessed by using R. Cells were always counted at the dorsomedial and dorsolateral regions of the adult zebrafish telencephalon ventricular zone.



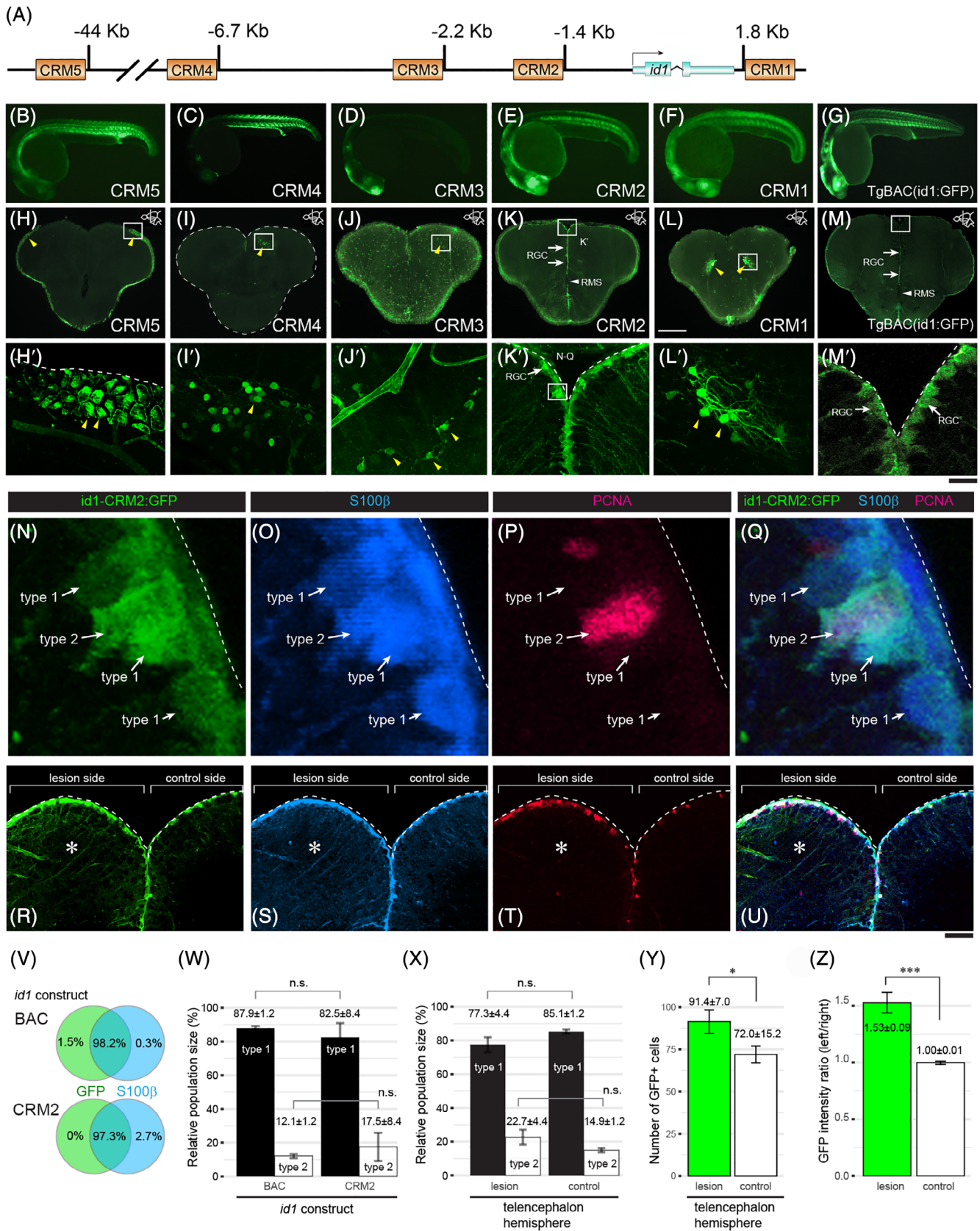


FIGURE 1 Legend on next page.

## 2.9 | Quantitative real-time PCR

Total RNA was isolated from adult telencephala using Trizol (Life Technology). First-strand cDNA was synthesized from 1 µg of total RNA with the Maxima First-strand cDNA synthesis kit (Thermo Scientific) according to the manufacturer's protocol. A StepOnePlus Real-Time qRT-PCR system (Applied Biosystems) and SYBR Green I fluorescent dye (Promega) were used. Expression levels were normalized using  $\beta$ -actin (Figure 7). The relative levels of mRNA were calculated using the  $2^{-\Delta\Delta CT}$  method. The primer sequences are listed in Table S2.

## 2.10 | RNA sequencing and library preparation

For RNA sequencing, total RNA was isolated from three injured hemispheres (5 days postinjury) and three uninjured contralateral telencephalic hemispheres each to create injured and uninjured RNAseq libraries, respectively. Our data were generated from three biological repeats (as described in Reference 25). Two milligrams of total RNA was used to prepare each of the six mRNAseq libraries. RNA sequencing data were retrieved from a previous data set.<sup>25</sup> The data analysis was carried out as described<sup>31</sup> using the latest version of the zebrafish reference genome, assembly GRCz11 ([https://www.ncbi.nlm.nih.gov/assembly/GCA\\_000002035.4/](https://www.ncbi.nlm.nih.gov/assembly/GCA_000002035.4/)).

## 3 | RESULTS

### 3.1 | Identification of a CRM mediating expression of *id1* in adult NSCs

To elucidate the mechanisms underlying *id1* expression in adult NSCs and its injury-induced upregulation, we performed a systematic search for CRMs controlling expression of *id1* in the ventricular zone of the adult telencephalon. Via phylogenetic sequence

comparison of the *id1* locus, we identified five conserved putative cis-regulatory modules (CRM1-5) upstream and downstream of the *id1* coding sequence (Figure 1A). The identified conserved noncoding sequences were inserted in front of a *gata2* minimal promoter,<sup>32</sup> coupled to a GFP reporter cassette<sup>28</sup> and introduced into the germ line of zebrafish to generate stable transgenic lines, *Tg(id1-CRMX:GFP)*, where X represents one of the five CRMs (Figure 1B-F, H-L, and H'-L'). All five CRMs mediated expression in 24-hour postfertilization (hpf) zebrafish embryos in somewhat overlapping but distinct and specific patterns (Figure 1B-F). In the adult telencephalon (Figure 1H-L and H'-L'), only *id1-CRM2* mediated specific GFP expression in the ventricular zone (white arrows, Figure 1K and Movie S1) in a pattern identical to the previously described GFP-tagged *id1* BAC (bacterial artificial chromosome) transgenic line, *TgBAC(id1:GFP)*<sup>25</sup> (Figure 1M and M'), while CRM5 (Figure 1H), CRM4 (Figure 1I), CRM3 (Figure 1J), and CRM1 (Figure 1L) drove ectopic GFP expression presumably at the tela choroidea and blood vessels (white rectangle, Figure 1H, magnification in 1H'), in neurons (white rectangle, Figure 1I, L and respective magnification in Figure 1I' and 1L') and in blood vessels and presumptive oligodendrocytes/neurons (white rectangle, Figure 1J and magnification in 1J'). The ventricular GFP-positive cells resembled RGCs in morphology and coexpressed the RGC marker *S100 $\beta$*  (96.9%  $\pm$  2.3%), (Figure 1K, K', N, Q, and R) which were shown to be the NSCs in the adult zebrafish telencephalon.<sup>9,10</sup> GFP was predominantly expressed in *S100 $\beta$ <sup>+</sup>/PCNA<sup>-</sup>* type 1 cells (82.5  $\pm$  8.4%,  $n = 3$  telencephala; Figure 1N-Q and R-U), while only a small number of GFP<sup>+</sup>/*S100 $\beta$ <sup>+</sup>* cells represented type 2 cells coexpressing PCNA (17.5  $\pm$  8.4%,  $n = 3$ ), a marker for cell proliferation. GFP expression was also excluded from the rostral migratory stream (RMS), a highly proliferative domain in the telencephalon composed of type 3 progenitors (Figure 1K, white arrowhead). These data show that GFP<sup>+</sup> cells correspond in majority to quiescent type 1 RGCs. Furthermore, both GFP expression and intensity were increased in the left telencephalic hemisphere upon stab injury compared to right noninjured control hemispheres (Figure 1R, U, V-W, and Y-Z). After stab wounding the

**FIGURE 1** The *id1* cis-regulatory module 2 (CRM2) drives ventricular expression and responds with increased expression to stab injury of the adult zebrafish telencephalon. A, Homology-based search for cis-regulatory modules (CRMs). Schematic representation of the *id1* locus with putative CRMs 1 to 5 highlighted by yellow rectangles. B-M', Stable GFP reporter expression of *id1*-CRM5 (B and H-H'), *id1*-CRM4 (C and I-I'), *id1*-CRM3 (D and J-J'), *id1*-CRM2 (E and K-K'), *id1*-CRM1 (F and L-L') are shown in comparison with the control *TgBAC(id1:GFP)* (G and M-M') for 24 hpf embryos (B-G) and adult telencephala (H-M'). H-M, GFP reporter expression analyzed in transverse sections from the middle part of the adult telencephalon (location of section schematically indicated in the upper-hand right corner). The *Tg(id1-CRM2:GFP)* transgenic line (K) recapitulates GFP expression of the *TgBAC(id1:GFP)* line (M) with strong expression in the ventricular zone (white arrows) and absence of expression in the rostral migratory stream (RMS, white arrowheads). The yellow arrowheads indicate ectopic GFP expression in the tela choroidea (H-H'), cells with appearances of neurons (I-I' and L-L') and oligodendrocytes (J-J'). Rectangles (H-M) represent the region magnified in H'-M', respectively. Dashed lines indicate the boundary of the telencephalon. N-Q, Magnified views of RGCs highlighting type 1 and type 2 RGCs identified by expression of *id1-CRM2:GFP* (N), *S100 $\beta$*  (O) and PCNA (P; all merged in Q). R-U, Transverse view of a 5 days postinjury telencephalon showing the expression of *id1-CRM2:GFP* (R), *S100 $\beta$*  (S) and PCNA (T; all merged in U). The lesion site (left hemisphere) is marked by an asterisk. V-W, Summary of colocalization analysis of GFP and *S100 $\beta$*  expression for BAC and CRM2-*id1* constructs. W, Relative population sizes of type 1 and type 2 RGCs for BAC and *id1-CRM2* constructs. X, Y, Relative population sizes of type 1 and type 2 RGCs (X) and the number of GFP<sup>+</sup> cells (Y) for *id1-CRM2* constructs, comparing lesioned and unlesioned control hemispheres. Z, *id1-CRM2:GFP* intensity ratio between left and right hemispheres comparing undamaged telencephalon (control) and damaged telencephalon (lesion). Significance is indicated by asterisks: \*.01  $\leq P < .05$ ; \*\*\* $P < .001$ . n.s. = not significant. Scale bars = 200 µm (H-M), 20 µm (B-G; H'-M'), 2 µm (N-Q), and 25 µm (R-U)

proportion of GFP<sup>+</sup>/S100β<sup>+</sup>/PCNA<sup>-</sup> type 1 and GFP<sup>+</sup>/S100β<sup>+</sup>/PCNA<sup>+</sup> type 2 stem cells was not altered in the injured left hemisphere relative to the right uninjured side, which is similar to the endogenous *id1* gene and the *id1* BAC transgenic line.<sup>25</sup> Additionally, GFP was predominately found in quiescent cells (Figure 1W,X). Thus, the *id1*-CRM2 drives expression of GFP in the RGCs in a pattern identical to the endogenous *id1* gene, and this expression is inducible by injury.

### 3.2 | Fine-mapping of the regulatory sequences mediating expression in RGCs

In order to map the core regulatory region of the *id1*-CRM2 responsible for its specific activity in the RGCs of the telencephalic ventricular zone, a series of 5' and 3' overlapping deletion variants of the reporter construct were generated and analyzed in stable transgenic lines (Figure 2A and data not shown). The transcriptional activities of these mutant versions were first investigated by monitoring GFP expression in 24 hpf zebrafish embryos. We observed at least three independent transgenic lines per construct and only constructs driving strong GFP expression resembling *id1* embryonic expression were selected for further analysis in the adult brain (Figure 2A and data not shown).

The deletion construct designed as *id1*-CRM2-core which contains a 157 bp long stretch of the CRM2 sequence (Figure 2A, chr11:18,706,838-18,706,994) drove expression in the ventricular zone of the adult telencephalon (Figure 2B). Double labeling experiments of the transgenic line *Tg(id1-CRM2-core:GFP)* revealed that this shorter version of the CRM2 drives mainly expression in PCNA<sup>-</sup>, S100β<sup>+</sup> RGCs (Figure 2B-E and J), as observed for the endogenous *id1*,<sup>25</sup> *id1*-BAC:GFP and *id1*-CRM2 (Figure 1R,U,V). Moreover, this short sequence responded to injury by increased expression and intensity of GFP (Figure 2F-I,L,M; n = 3 telencephala). Thus, our deletion approach led to the identification of a 157 bp sequence that appears to harbor all relevant sequences to drive expression in NSCs and to respond to injury. Remarkably, this sequence also proved sufficient to drive GFP expression in the brain, eye, somites, midline and urogenital opening in 24 hpf embryos (Figure S1) indicating that both embryonic and adult regulatory signals act through this CRM.

### 3.3 | *Id1*-CRM2-core is structurally and functionally conserved between fish and human

Sequence analysis of zebrafish *id1*-CRM2-core with the *MatInspector* software<sup>33</sup> showed that this regulatory module harbors TF binding sites for Forkhead box protein A2 (FoxA2), cyclic AMP response element binding protein (CREB), Homeobox domain transcription factor (Pknx), and Early growth response gene 1 (Egr1), as well as two *smad binding motifs* (SBMs) (Figure 3A). The entire core sequence displays a high degree of conservation between

zebrafish, mouse, and human homologues. We thus tested whether the sequence is also functionally conserved by constructing a transgene harboring the human version of the zebrafish CRM2-core referred to as *Hsid1*-CRM2-core. After stably introducing this transgene into the germ line of zebrafish, we analyzed expression in the adult telencephalon (Figure 3B-E). The human sequence also mediated expression in the ventricular zone, in type 1 progenitors corresponding to quiescent RGCs (PCNA<sup>-</sup>, S100β<sup>+</sup>), similar to the zebrafish sequence (Figures 3J and 2J, respectively). Moreover, when a brain injury was inflicted in one hemisphere of the telencephalon the *Hsid1*-CRM2-core carrying transgene also responded to the stab wound by increased expression at 5 days postlesion (dpi) (Figure 3F-I,L,M; n = 3 telencephala). Taken together, these results show that the mechanism of *id1* regulation appears to be conserved from fish to human, suggesting that the mechanisms underlying the control of neurogenesis are very similar despite the remarkably different abilities to repair lesions in the adult brain among these phylogenetically distant vertebrate species.

### 3.4 | BMP response elements are required for *id1*-CRM2 activity in the zebrafish adult telencephalon

The central region (chr11:18,706,875-18,706,953) of the *id1*-CRM2-core, situated between the *foxA2* and *egr1* binding sites and containing two SBMs (Figures 3A and 4A), is similar to a previously identified *BMP response element* (BRE) of the mouse and human *id1* gene<sup>34,35,36</sup>. Because *id1* is a direct target of the BMP signaling pathway<sup>37</sup> and smads transduce the BMP signal from the cytoplasm to the nucleus<sup>38</sup> (Figure 6A), we tested whether this BRE is necessary for the function of *id1*-CRM2 in the zebrafish adult telencephalon. To this aim we generated two *id1*-CRM2 mutant variants, in which either the conserved 74 bp sequence covering the BRE was deleted (*id1*-CRM2-Δ74) (Figure 4B) or both SBM1 and SBM2 sequences were mutated (*id1*-CRM2-mut-SBMs) (Figure 4C). GFP expression in the ventricular zone and in RGCs was abolished in transgenic lines carrying the mutant constructs (Figure 4D-H [*id1*-CRM2-Δ74; no GFP, expression in S100β<sup>+</sup> cells n = 5]) and (Figure 4I-M [*id1*-CRM2-mut-SBMs, no GFP expression in S100β<sup>+</sup> n = 6]) and no induction of GFP expression upon injury could be detected for both constructs (Figure S3). These results show that the BRE located in the *id1*-CRM2 is critical for the expression of *id1* in RGCs. Moreover, they suggest that BMP signaling may play a role in controlling *id1* expression in the telencephalon of the adult zebrafish.

We next tested whether the well-characterized mouse *id1* BRE<sup>34,35</sup> that contains multiple SBMs would control expression in the telencephalon. A construct containing two tandem copies of the mouse BRE was shown to mediate GFP expression in all BMP signaling target tissues of zebrafish embryos.<sup>39,40</sup> Surprisingly, however, it did not show any activity in the RGCs of the ventricular zone of the adult telencephalon (Figure 4O), and was unaffected by brain injury (Figure 4P,Q). In the transgenic line *Tg(BRE:GFP)*, GFP expression is



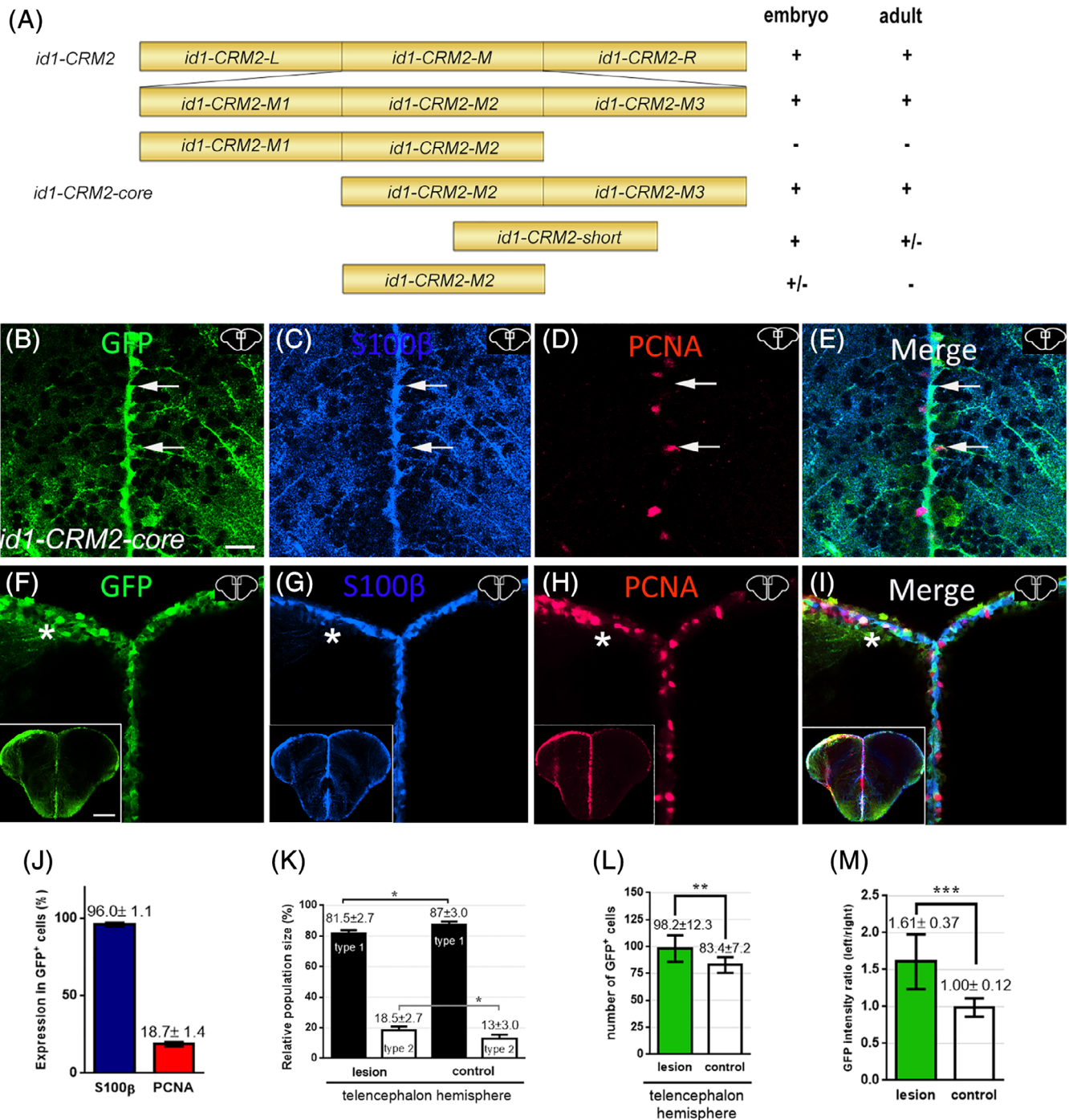


**FIGURE 2** Deletion mapping of *id1-CRM2* identified a 157 bp core region, which confers RGC-specific expression in the adult telencephalon. A, 5' and 3' deletions of *id1-CRM2* analyzed for expression in zebrafish embryos and adult brains. Results are summarized on the right; + indicates specific GFP expression; ± and - represent weak and absence of expression, respectively. B-I, Immunohistochemistry of telencephalic transverse sections with antibodies against GFP (B, F), S100β (C, G), and PCNA (D, H) (merged panels: E, I). Section levels and areas of magnification are indicated in the upper right-hand corner of each image. B-E, White arrows show two RGCs. E, The upper cell is GFP<sup>+</sup>/S100β<sup>+</sup>/PCNA<sup>-</sup> (type 1 RGC), whereas the lower cell is GFP<sup>+</sup>/S100β<sup>+</sup>/PCNA<sup>+</sup> (type 2 RGC). F-I, Upon stab wound injury the reporter construct expression is upregulated. The left injured side is labeled with a white asterisk. B-I, Section levels and areas of magnification are indicated in the upper right-hand corner each image. J, Quantification of PCNA and S100β expression in *id1-CRM2:GFP*-positive cells. K, Relative population size of type 1 and type 2 RGCs in the control and lesioned hemisphere. L, M, Quantification of GFP-positive cells and GFP intensity upon injury. Graphs showing the number of GFP-expressing cells (L) and the intensity ratio between left uninjured (control) and right injured hemispheres respectively (M). Bars: mean ± SD. Significance is indicated by asterisks: \**P* < .05; \*\**P* < .01; \*\*\**P* < .001. Boxed image in lower left-hand corner of (F-I) represents entire brain sections. *n* = 3 animals (B-L), *n* = 15 sections (M). Scale bar = 20 μm (B-I); 200 μm for Boxed image in lower left-hand corner of (F-I)



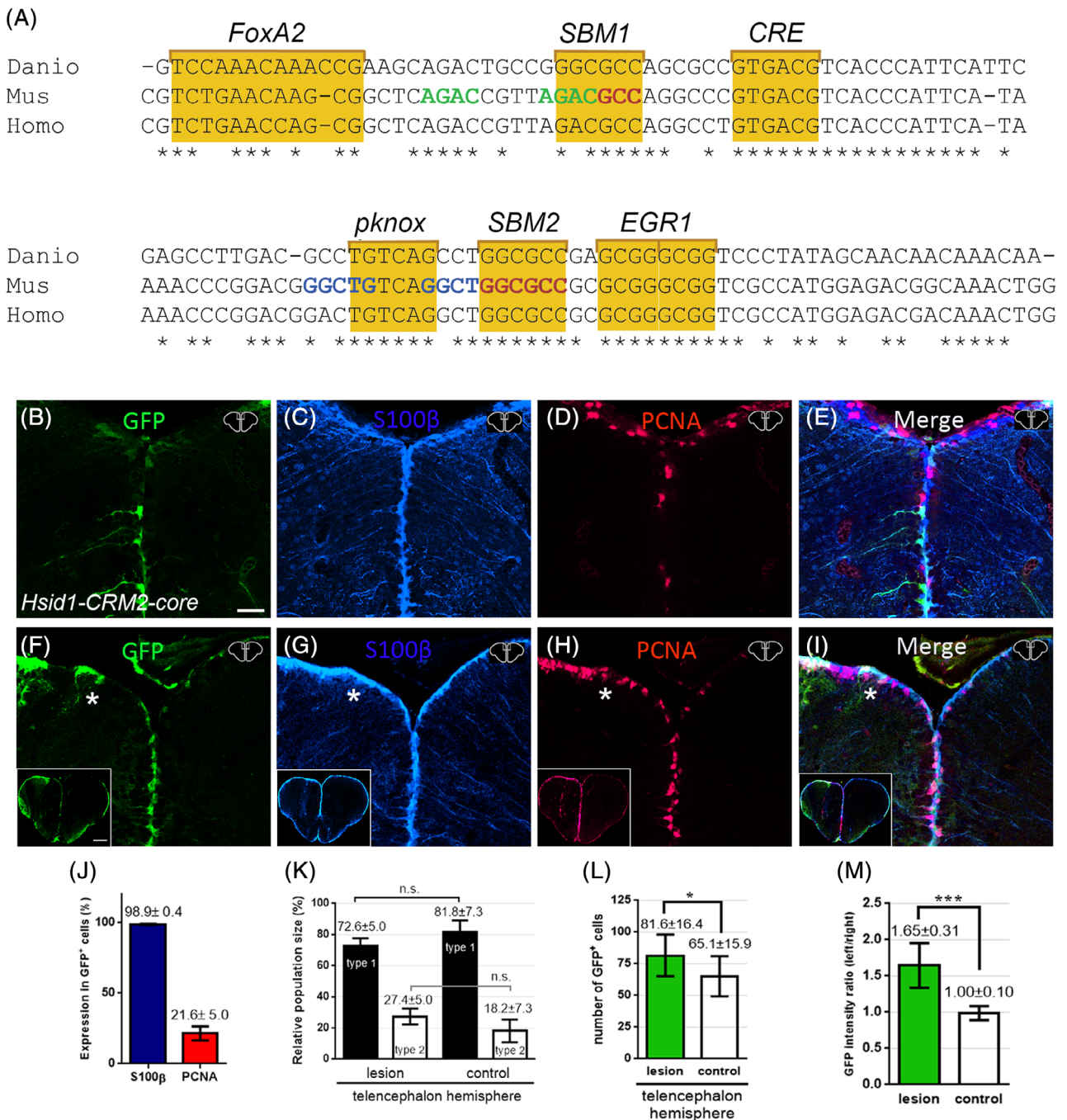


**FIGURE 3** Conservation of the zebrafish *id1-CRM2* core sequences and its function across evolution. A, Sequence comparison of zebrafish *id1-CRM2-core* (Danio) with human (Homo) and mouse (Mus) orthologous sequences. Conserved nucleotides are indicated with an asterisk. Conserved motifs are outlined by yellow boxes comprising putative DNA recognition sequences for the transcription factors FoxA2, Smad (SBM1 and 2), CRE binding protein (CREB), Pknox, and EGR1. Nucleotide sequences in green, red, or blue correspond to previously identified sequences in the mouse *id1* orthologue: *Smad binding element* (SBE), a Smad 1/5 binding site and a binding site for an unknown binding protein, respectively. B-I, Immunohistochemistry of telencephalic transverse sections with antibodies against GFP (B, F), S100β (C, G), and PCNA (D, H) (merged panels: E, I). B, Expression of GFP in RGCs at the telencephalic ventricular zone driven by the human *id1* regulatory sequences in the zebrafish adult telencephalon. F, Expression of the human *Tg(Hsid1-CRM2)* driven reporter construct is upregulated upon stab wound injury. The injured telencephalic hemisphere is labeled with a white asterisk. J, Quantification of PCNA and S100β expression in GFP<sup>+</sup> cells in the *Tg(Hsid1-CRM2)* line. K, Relative population size of type 1 and type 2 RGCs in the control and lesioned hemispheres. The proportion of GFP<sup>+</sup>/S100β<sup>+</sup>/PCNA<sup>-</sup> type 1 and GFP<sup>+</sup>/S100β<sup>+</sup>/PCNA<sup>+</sup> type 2 stem cells is not altered in the injured hemisphere relative to the control hemisphere of the telencephalon. L, M, Quantification of GFP<sup>+</sup> cells upon injury. The number of GFP-expressing cells (L) and the intensity ratio between left and right hemispheres comparing undamaged hemisphere (control) and damaged telencephalic hemisphere (M) are both increased following injury. Bars: mean ± SD. Significance is indicated by asterisks: \* $.01 \leq P < .05$ ; \*\*\* $P < .001$ . n.s. = not significant. Boxed in image in lower left-hand corner of (F-I) represents entire brain sections.  $n = 3$  animals (B-L),  $n = 15$  sections (M). Scale bar = 20 μm (B-I); 200 μm for boxed image in lower left-hand corner of F-I

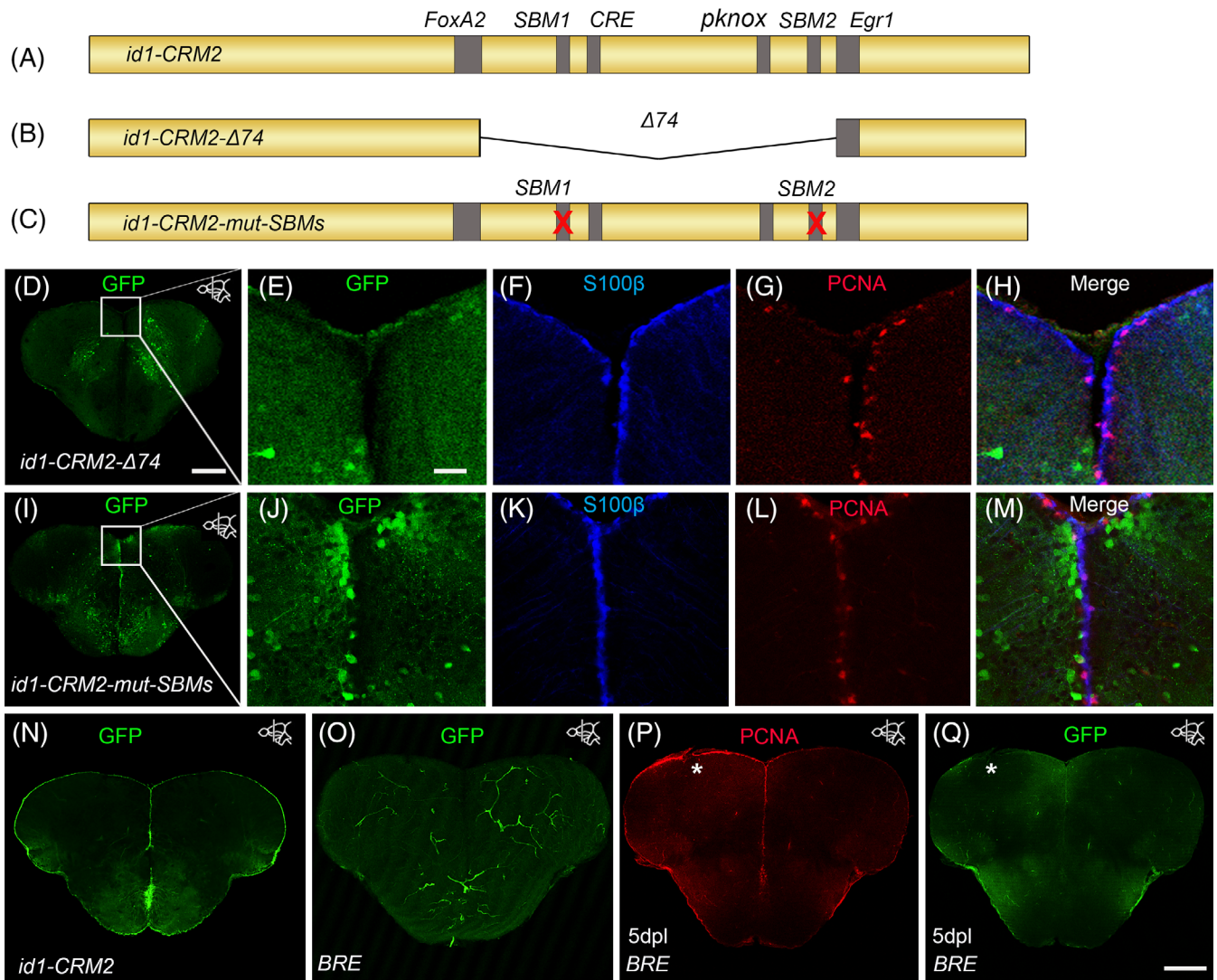


**FIGURE 4** The conserved BMP response element in the *id1-CRM2* is crucial for correct expression of the GFP reporter in the ventricular zone and RGCs. A-C, Scheme showing mutated *id1-CRM2* reporter constructs: A, *id1-CRM2* wt construct with putative TF binding sites indicated in gray. B, *id1-CRM2-Δ74* construct which contains a deletion of a 74 bp stretch of the most conserved sequence in *id1-CRM2*. C, *id1-CRM2-mut-SBMs* construct with mutations in the 2 SBMs (1 and 2) of *id1-CRM2*. D, Deletion of the 74 bp stretch in the *id1-CRM2* abolished GFP expression in the ventricular zone. E-H, Enlarged micrographs of D. E-H, Immunohistochemistry with GFP (E), S100β (F), and PCNA (G) antibodies on telencephalic cross sections of the *id1-CRM2-Δ74* transgenic line shows no GFP reporter expression in S100β<sup>+</sup> RGCs (H, merged view). I-M, Mutations in *Smad binding motifs* (SBM1 and 2) abolished GFP expression in the ventricular zone. J-M, Magnification of white-boxed region in I. J-M, Immunohistochemistry with GFP (J), S100β (K), and PCNA (L) antibodies on telencephalic cross sections of the *id1-CRM2-mut-SBMs* transgenic line show no colocalization between the RGC marker, S100β, and GFP (M, merged view). N, GFP expression driven by *id1-CRM2:GFP* reporter construct in the ventricular zone (control). O, P, Q Immunohistochemistry of telencephalic cross sections with GFP (O, Q) and PCNA (P). O, Q, The *BRE* does not drive GFP expression in the RGCs (O) and is not inducible by telencephalic injury (Q). The left injured side is labeled with a white asterisk. Anteroposterior positions of transverse sections are indicated in the upper right-hand corner of each image. Scale bar = 20 μm (E, F, G, H, J, K, L, M); 200 μm (D, I, N, O, P, Q)

restricted to blood vessels of the adult brain (Figure 4O, n = 7), in contrast to the expressions driven by *id1-CRM2* (Figure 4N) and *id1-CRM2-core* (Figure 2B), which are RGC-specific (compare Figure 4N with Figure 4O). This blood vessel expression was observed with two independent lines of the *BRE:GFP* described in References 39 and 41. These findings suggest that in the adult zebrafish brain, the BMP pathway alone is critical but not sufficient to drive *id1* expression in the ventricular RGCs.

### 3.5 | BRE and additional transcription factors are necessary for full activity of *id1-CRM2* in NSCs

The observation that the two tandem copies of the mouse *BRE*<sup>34</sup> are not sufficient to drive reporter gene expression in RGCs (Figure 4O) suggests that further sequences are required in addition to *SBMs* for activity of *id1-CRM2-core* in RGCs. Indeed, the *id1-CRM2-core* contains several other well-conserved binding sites for transcription



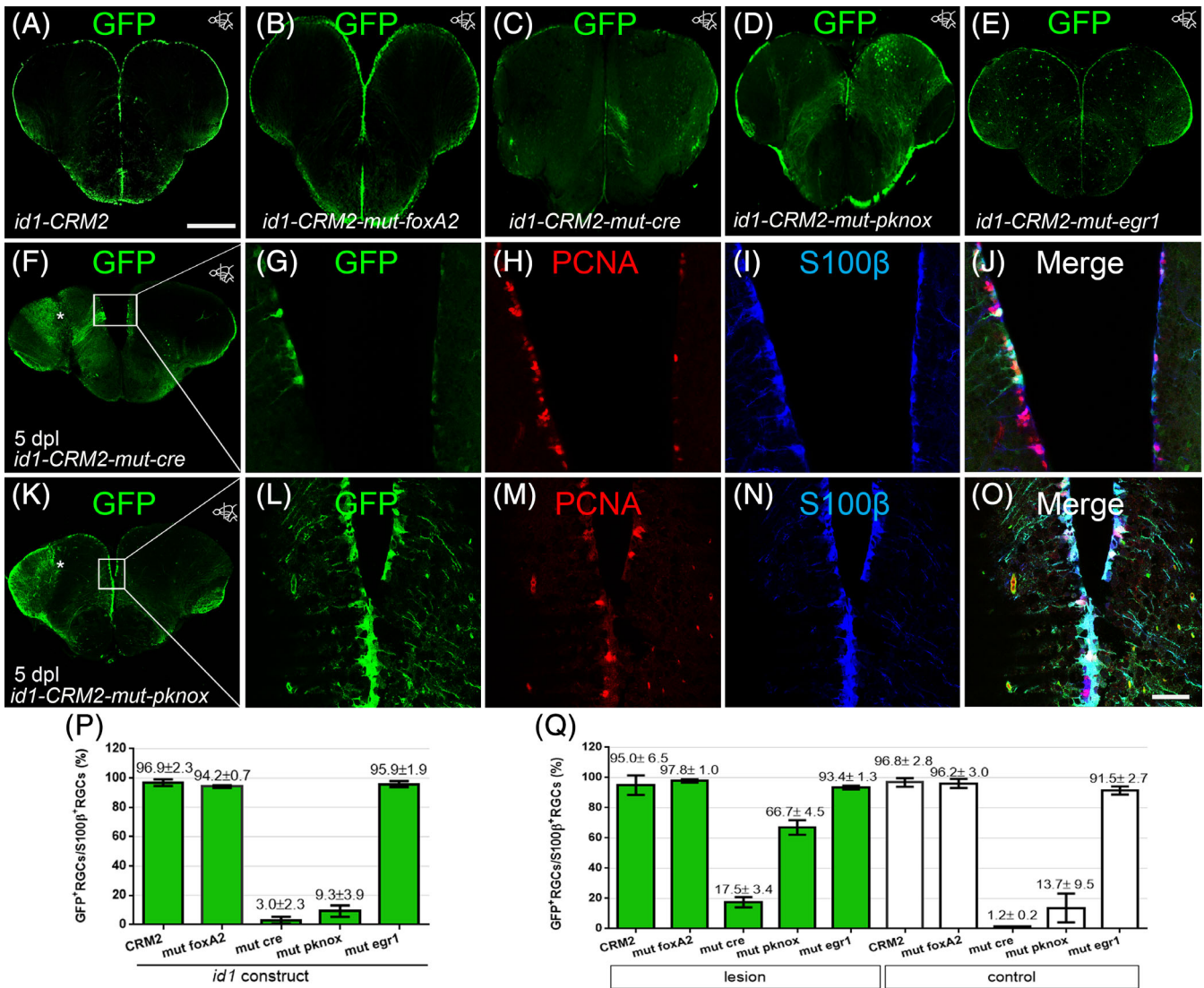


**FIGURE 5** Cre and pknx binding sites in close vicinity to SBM1 and – 2 are necessary for the full activity of *id1-CRM2*. A-E, Immunohistochemistry with a GFP antibody on telencephalic cross sections of the *id1-CRM2* transgenic lines containing a mutation in the *foxA2* (B), *cre* (C), *pknx* (D), and *egr1* (E) binding sites, respectively. Mutation in *cre* (C) and *pknx* (D) binding sites leads to a reduction of GFP<sup>+</sup> cells in the ventricular zone. F, G, J, Expression of the *id1-CRM2-mut-cre* construct is inducible by brain injury (white asterisk, left injured hemisphere). G-J, Magnification boxed area in F. K, L, O, Expression of the *id1-CRM2-mut-pknx* construct is induced upon brain injury (white asterisk, left injured hemisphere). L-O, Magnification of boxed area in K. Anteroposterior positions of transverse sections are indicated in the upper right-hand corner of each image. P, Q, Percentage of GFP<sup>+</sup>/S100<sup>β</sup><sup>+</sup> RGCs over the total number of S100<sup>+</sup> RGCs for *id1-CRM2* mutant constructs under homeostatic condition (P) and at 5 days postinjury, comparing the injured hemisphere (green columns) and the contralateral uninjured hemisphere (white columns; Q) at the dorsomedial to the dorsolateral region of the telencephalon. Scale bar = 200 μm (A-F and K); 25 μm (G-J and L-O)

factors surrounding the SBMs (Figure 3). To test whether these neighboring sequences are necessary in addition to the BRE, each of these sites was individually mutated, and stable transgenic lines were generated with the resulting mutant constructs (Figure 5A-E). While mutation in the *foxA2* and *egr1* binding sites had no effect on the expression pattern of GFP in the RGCs of the adult brain (Figure 5B,E, P,Q), we observed a reduction in GFP expression for constructs with mutated *pknx* or *cre* binding sites (Figure 5C,D,P,Q). Notably, we still observed a strong and specific response to stab injury of the telencephalon in these two mutant lines (Figure 5F-J,P,Q and Figure 5K-O, P,Q). This finding indicates that these sites together with SBMs are

necessary for RGC-specific expression. However, since mutations of the individual *cre* (Figure 5F-J,P,Q) and *pknx* (Figure 5K-O,P,Q) sites did not affect the capacity to respond to injury, these sites appear not to be required for injury-induced expression via the BMP pathway.

### 3.6 | *id1-CRM2* expression is induced by the BMP pathway in response to injury

A crucial question is whether the increase in *id1-CRM2* mediated transcription at the ventricular zone upon injury involves BMP signaling,

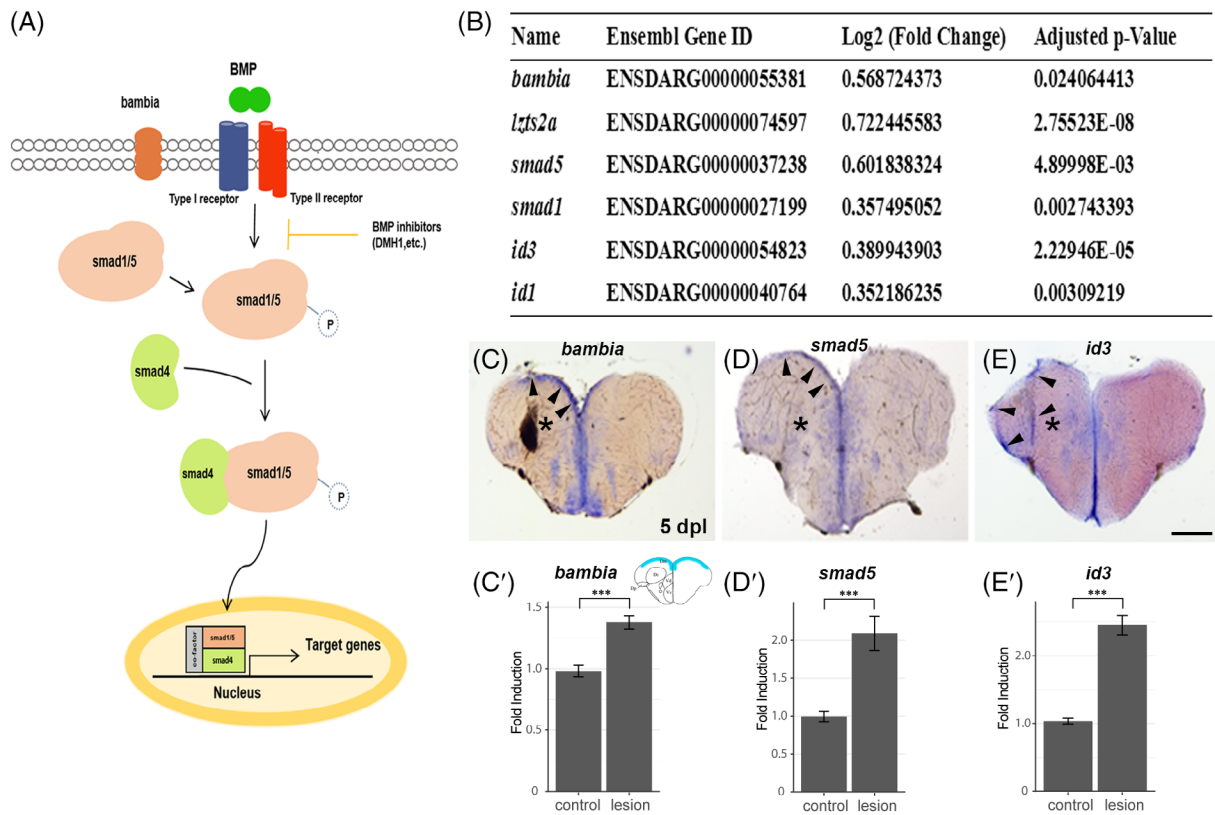


**FIGURE 6** Genes involved in canonical BMP signaling are induced in response to telencephalic injury. A, Scheme of the BMP signaling pathway. B, RNAseq analysis of injured telencephala hemispheres in comparison to uninjured hemispheres reveals an upregulation in mRNA expression of BMP signal transducers (*smad5*), regulators (*bambia*) or downstream target genes (*id3*, *id1*). C-E, In situ hybridization on sections of the adult zebrafish telencephalon 5 days postlesion. C, *bambia*, D, *smad5*, E, *id3*. Arrowheads indicate upregulation of gene expression in the left telencephalic hemisphere upon stab injury. C'-E', Quantification of C'*bambia*, D', *smad5*, and E', *id3* expression upregulation 5 days postlesion. Only upregulated areas were quantified along the control and injured ventricular zone from the dorsomedial to the dorsolateral region of the telencephalon (scheme in the upper right-hand corner of (C')) shows the quantified area in blue). Significance is indicated by asterisks: \*\*\*P < .001. P-values: *bambia*: 0.00008917 (C'), *smad5*: 0.003684 (D'), *id3*: 7.455 x 10<sup>-7</sup> (E'). Scale bar = 200 μm (C, D, E)

as suggested by the requirement of the BRE for CRM2 activity. To address this question, in a first step we analyzed deep sequencing data sets of the transcriptomes generated from 5 days postlesion (dpl) hemispheres vs contralateral noninjured adult zebrafish telencephala.<sup>25</sup> We discovered an increase in the transcription levels of several key genes involved in canonical BMP signaling (Figure 6A,B) when compared to the control, uninjured side. Among those, we identified the *BMP receptor1aa* (*bmp1aa*), the BMP receptor specific signal transducers *smad1* and *smad5* as well as several direct target genes of BMP signaling, including *id1*, *id3*, *izts2a* and *bambia* (Figure 6B). For genes that are significantly upregulated (Figure 6B) and that display a restricted pattern of expression in the telencephalon under homeostatic conditions (*bambia*, *smad5* and *id3*), the results were further verified by in situ hybridization (ISH) on telencephalic cross sections at 5 dpl (Figure 6C-E). A distinct upregulation of *bambia*, *smad5*, and *id3* at 5 dpl in the injured left telencephalic hemisphere was detected on the sections when compared to the right uninjured hemisphere, where expression did not change (Figure 6C-E; n = 4 telencephala per gene). The RNA sequencing and ISH data were confirmed by quantifying the

staining intensity of *bambia*, *smad5* and *id3* following brain injury at 5 days postlesion at the injury site in comparison to the same region in the intact contralateral control hemisphere (Figure 6C'-E').

To functionally manipulate BMP signaling during the response to injury, telencephala of adult fish were injured on the second day of treatment with 20 μM of the BMP signaling pathway inhibitor DMH1 (dorsomorphin homologue 1<sup>42,43</sup>). The fish were analyzed at 5 dpl. As visualized by in situ hybridization (Figure 7A,B,D,E) and by qPCR analysis (Figure 7C,F), suppression of BMP signaling by exposure to DMH1 led to a significant loss of induction of the endogenous *id1* gene (Figure 7B) and *id1*-CRM2:GFP reporter gene (Figure 7E) upon injury of the telencephalon. We also observed a strong reduction in the basal expression of the *gfp* transgene and *id1* endogenous gene in the uninjured telencephalic hemispheres upon DMH1 treatment (Figure 7C,F).

In summary, our investigation of the transcriptional regulation mediated by *id1*-CRM2 suggests that BMP signaling positively regulates the expression of *id1* in the adult zebrafish brain during constitutive and regenerative neurogenesis.



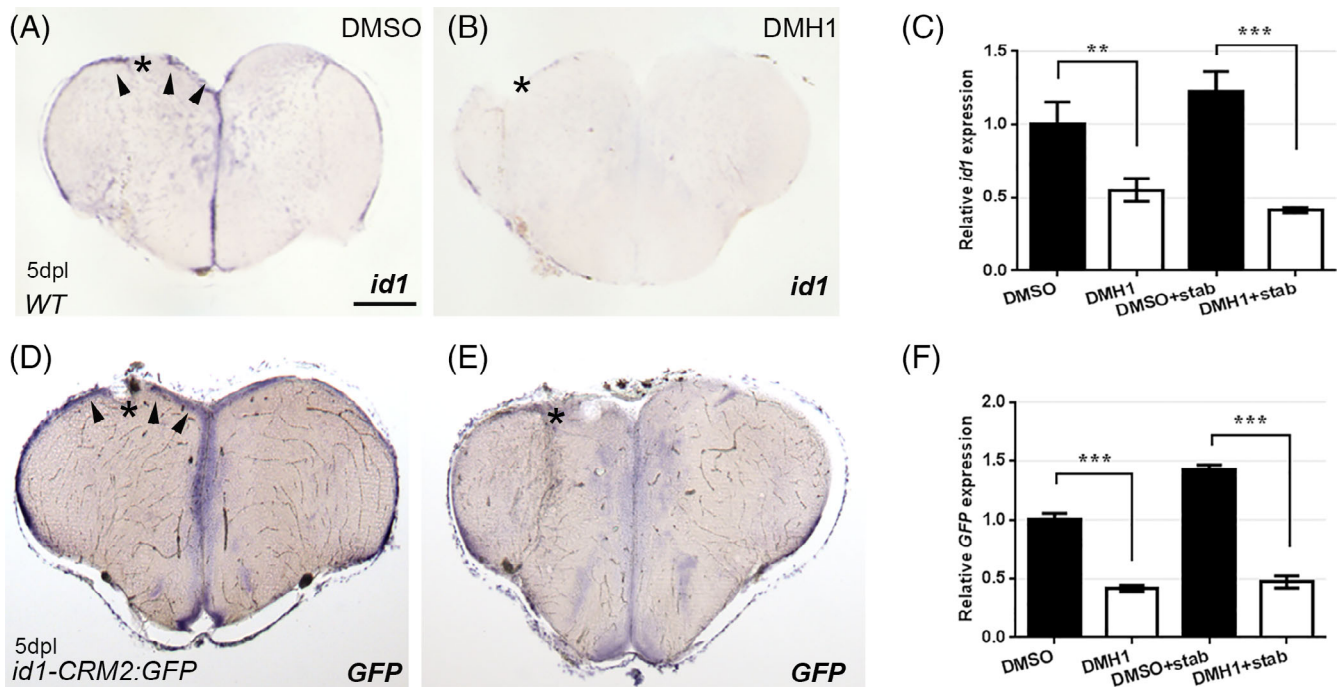


**FIGURE 7** Inhibition of BMP signaling with DMH1 reduces injury-induced *id1* and *id1-CRM2:GFP* transgene expression. ISH against *id1* (A, B) and *gfp* mRNA (D, E) showed reduction in induction of *id1* (B) and *gfp* (E) transgenes upon BMP signaling inhibition by DMH1 treatment (B and E) in comparison to DMSO-treated corresponding controls (A and D). Arrowheads indicate upregulation of gene expression the left telencephalic hemisphere upon stab injury. C, F, RT-qPCR quantification confirmed reduction in *id1* and *gfp* expression in DMH1 treated fish. The data represent the mean  $\pm$  SD of three independent experiments. Significance is indicated by asterisks: \*\* $.001 \leq P < .01$ ; \*\*\* $P < .001$ . Scale bar = 200  $\mu$ m (A, B, D, and E).  $n = 3$  animals for C, F

## 4 | DISCUSSION

Here, we identified the DNA module *id1-CRM2* as a key regulator of *id1* expression in the ventricular zone of the adult zebrafish telencephalon. Moreover, we show that a *BRE* is crucial for the activity of this CRM and that inhibition of BMP signaling reduces expression of the CRM driven reporter, both during constitutive and reactive neurogenesis. This requirement of BMP signaling is correlated with an increase in mRNAs encoding BMP pathway components and BMP-controlled genes in the transcriptome of injured telencephala.

### 4.1 | BMP as a regulator of *id1* expression during constitutive and regenerative neurogenesis

A key question is which cues control *id1* expression in RGCs during constitutive and regenerative neurogenesis. Inflammatory signals were previously implicated in the induction of regenerative neurogenesis in the zebrafish telencephalon.<sup>44</sup> However, *id1* expression was not affected by inflammation.<sup>25</sup> Additionally, Notch signaling, previously shown to be involved in the control of neurogenesis in the zebrafish,<sup>45,46</sup> did not affect *id1* expression, either.<sup>25</sup> Our systematic deletion and mutation analysis of the CRM2 module, as well as pharmacological inhibition of the BMP/Smad signaling pathway strongly suggest that BMP signals are crucial for *id1* expression in the adult

zebrafish telencephalon during both constitutive and regenerative neurogenesis. The observation that BMP signaling components (*bmp1aa*, *smad1*, *smad5*), as well as known BMP-controlled genes such as *bambia*, *id3*, and *lzts2a* are induced upon brain lesion in addition to the *id1* gene suggests that injury increases the basal level of BMP signaling in the telencephalon.

Remarkably, injury-induced proliferation of NSCs and upregulation of BMP target genes are always restricted to the injured side of the telencephalon (eg,<sup>20,25</sup> and this study). Given the close juxtaposition of left and right hemispheres in the medial parts of the telencephalon, this restriction of induction in gene expression and proliferation to the injured half is rather remarkable and implies a highly limited diffusion of the BMP signals toward the uninjured hemisphere. Rather than diffusing freely within the injured side, BMP signals may be sensed and relayed down to the cell bodies at the ventricular zone by the long processes of the RGCs. *Bmp2*, *bmp4*, and *bmp7* mRNAs are expressed in the telencephalon (unpublished data), but the type of BMP signals involved in injury response as well as their origin are unclear. Although, we detected mRNA expression of these *bmps* in our transcriptome data, the change in response to injury was not significant. We did also not observe a reduction in the expression of BMP signaling inhibitors, such as *smad6*, *smad7*, *noggin*, and *folistatin* genes (data not shown). Therefore, it is tempting to speculate that the lesion triggers either release of BMPs or their maturation.

## 4.2 | BMPs as regulators of quiescence and proliferation of NSCs in reactive neurogenesis

In agreement with our data, previous work in mouse associated BMP signaling and *id* genes with maintenance of the adult NSCs of the hippocampus and lateral ventricle during constitutive neurogenesis.<sup>47-49</sup> However, in mice the situation is more complicated as several *id* genes act redundantly.<sup>49</sup> A single *id* gene appears to provide this function in the zebrafish.<sup>25</sup>

Here, we provide evidence that the mechanism of neural stem cell maintenance by *id1* is conserved not only in constitutive adult neurogenesis, as observed in mouse, but also in the teleost-specific reactive neurogenesis, which is involved in injury repair. BMP signals appear to play a crucial role in elevating *id1* expression in response to injury and in this way to eventually downregulate proliferation of RGCs, securing a pool of resting stem cells for future activation. In this context, it is important to stress that *id1* expression reacts in a delayed fashion relative to the induction of proliferation.<sup>25</sup> Another signaling system maintaining adult neural stem cell quiescence is the Notch pathway in both zebrafish and mice.<sup>45,50</sup> It remains to be assessed whether the BMP/*Id1* and Notch/*Her4.1* pathways are redundant or parallel pathways with distinct functions in stem cell maintenance during constitutive and reactive neurogenesis. In mouse it was recently suggested that both Notch/*Hes* and *Bmp/Id* pathways interact to enhance quiescence of NSCs.<sup>51,52</sup>

## 4.3 | *Id1-CRM2* is structurally and functionally highly conserved

*Id1-CRM2* is a highly conserved CRM with homologous sequences in all-vertebrate species examined so far (this report,<sup>53</sup>). The 74 bp central region of *id1-CRM2-core* situated between the *foxA2* and *egr1* binding sites is very similar to a previously identified *BRE* of the mouse and human *id1* regulatory sequence.<sup>34,35</sup> The two zebrafish *SBM1* and *SBM2* located in the central region perfectly match the *smad* binding site consensus GGC GCC<sup>54,55</sup> and that of the *smad binding element (SBE)*, AGAC<sup>56,57</sup>. These elements are critical for BMP-induced *id1* expression in the mouse C2C12 myoblast cell line<sup>34</sup>. Transgenes harboring tandem copies of this central *BRE* served as reliable reporters of canonical BMP signaling activity in mice and zebrafish embryos.<sup>39,40,58,59</sup>

However, this region was found to be necessary but not sufficient in *id1-CRM2* to drive expression of *id1* in RGCs of the adult zebrafish telencephalon. Moreover, the tandem copy of the *BRE* did not mediate expression in RGCs of the telencephalon. Conserved *cre* and a *pknox* site were found to be necessary in addition to the *BRE* core of *id1-CRM2* for basal expression in the RGCs. The combination of *smad* binding sites with *cre* is a conserved feature of the *id1-CRM2*, which is shared with many other BMP target modules in the mammalian genome.<sup>60</sup> In mouse osteoblasts, a cAMP response element was shown to enhance the response of *id1* to BMP signals,<sup>61</sup> showing that this interaction is not only restricted to

NSCs in the zebrafish but is also employed during bone formation in mammals.

The *pknox* binding site in the *id1-CRM2* partially overlaps with the *BRE* sequences (CGCC, CAGC) identified in mouse *id1* to be necessary for strong responsiveness to BMP signaling.<sup>34</sup> Therefore, it may be possible that these mutations impair the *BRE*. However, the mutations of the *pknox* and *cre* sites did not impair the BMP mediated response to injury. Our data suggest that their function is dispensable for BMP mediated induction of *id1* reporter expression in response to injury, suggesting that basal and induced expression may involve different cofactors.

Taken together this regulatory region of the *id1* gene appears to be structurally highly conserved between fish and mammals and serves as a regulatory interface that integrates multiple inputs. The high structural conservation is reflected by the fact that the human sequence can drive expression in RGCs of the adult zebrafish telencephalon. Remarkably, this conservation of function is not restricted to constitutive neurogenesis, but the human sequence also faithfully reproduces the response to injury. Thus, despite the vast difference in regenerative capacity, the underlying basic mechanism of reactive neurogenesis appears to be conserved between fish and mammals. This underscores the value of studies in the zebrafish as a model to develop therapies for injuries of the human brain. Clearly, *id1-CRM2* is a highly versatile CRM that drives expression in the zebrafish embryo in various tissues including the notochord<sup>53</sup>. It is thus expected to contain other elements, some of which may not reveal themselves by conserved sequence homology.<sup>53</sup>

## 5 | CONCLUSION

Here, we have identified an RGC CRM of *id1*, which mediates the input from the BMP signaling pathway into the adult NSCs during constitutive and regenerative neurogenesis in the zebrafish telencephalon. This CRM has a high potential to serve as an interface, which will permit to alter the balance between proliferation and maintenance of stem cells in experimental, as well as medical applications.

## ACKNOWLEDGMENTS

We thank Nadine Borel and the fish facility staff for fish care, Sabrina Weber for technical support, Maryam Rastegar for her support with the microscopes, and Thomas Dickmeis for proofreading of the manuscript, Salim Seyfried, Elise Cau, Natascia Tiso, and Matthias Hammerschmidt for sharing zebrafish transgenic lines. We are grateful for support by the EU IP ZF-Health (Grant number: FP7-242048), the Deutsche Forschungsgemeinschaft (GRK2039), the program Bio-Interfaces in Technology and Medicine of the Helmholtz foundation and the European Union's Horizon 3952020 research and innovation program under the Marie Skłodowska-Curie grant agreement No. 643062 (ZENCODE-ITN).

## CONFLICT OF INTEREST

The authors declared no potential conflicts of interest.

## AUTHOR CONTRIBUTIONS

S.R.: designed the experiments and supervised the work, analyzed the data, and wrote the manuscript; U.S.: analyzed the data, and wrote the manuscript; G.Z., M.F.: conducted the experiments and analyzed the data; L.L., T.B.: conducted the experiments; V.G.: performed the RNA sequencing data analysis; M.T., N.D.: analyzed and quantified the data.

## DATA AVAILABILITY STATEMENT

The data that support the findings of this study are available on request from the corresponding author.

## ORCID

Sevand Rastegar  <https://orcid.org/0000-0003-4411-5646>

## REFERENCES

1. Adolf B, Chapouton P, Lam CS, et al. Conserved and acquired features of adult neurogenesis in the zebrafish telencephalon. *Dev Biol*. 2006;295:278-293.
2. Grandel H, Kaslin J, Ganz J, Wenzel I, Brand M. Neural stem cells and neurogenesis in the adult zebrafish brain: origin, proliferation dynamics, migration and cell fate. *Dev Biol*. 2006;295:263-277.
3. Zupanc GK, Hinsch K, Gage FH. Proliferation, migration, neuronal differentiation, and long-term survival of new cells in the adult zebrafish brain. *J Comp Neurol*. 2005;488:290-319.
4. Alunni A, Bally-Cuif L. A comparative view of regenerative neurogenesis in vertebrates. *Development*. 2016;143:741-753.
5. Kizil C, Kaslin J, Kroehne V, Brand M. Adult neurogenesis and brain regeneration in zebrafish. *Dev Neurobiol*. 2012;72:429-461.
6. Lindsey BW, Hall ZJ, Heuze A, et al. The role of neuro-epithelial-like and radial-gliial stem and progenitor cells in development, plasticity, and repair. *Prog Neurobiol*. 2018;170:99-114.
7. Schmidt R, Strähle U, Scholpp S. Neurogenesis in zebrafish - from embryo to adult. *Neural Dev*. 2013;8:3.
8. Ganz J, Kaslin J, Hochmann S, Freudenreich D, Brand M. Heterogeneity and Fgf dependence of adult neural progenitors in the zebrafish telencephalon. *Glia*. 2010;58:1345-1363.
9. März M, Chapouton P, Diotel N, et al. Heterogeneity in progenitor cell subtypes in the ventricular zone of the zebrafish adult telencephalon. *Glia*. 2010;58:870-888.
10. Lam CS, März M, Strähle U. Gfap and nestin reporter lines reveal characteristics of neural progenitors in the adult zebrafish brain. *Dev Dyn*. 2009;238:475-486.
11. Pellegrini E, Menuet A, Lethimonier C, et al. Relationships between aromatase and estrogen receptors in the brain of teleost fish. *Gen Comp Endocrinol*. 2005;142:60-66.
12. Dray N, Bedu S, Vuillemin N, et al. Large-scale live imaging of adult neural stem cells in their endogenous niche. *Development*. 2015;142:3592-3600.
13. Rothenaigner I, Krecsmarik M, Hayes JA, et al. Clonal analysis by distinct viral vectors identifies bona fide neural stem cells in the adult zebrafish telencephalon and characterizes their division properties and fate. *Development*. 2011;138:1459-1469.
14. Diotel N, Vaillant C, Kah O, Pellegrini E. Mapping of brain lipid binding protein (Blbp) in the brain of adult zebrafish, co-expression with aromatase B and links with proliferation. *Gene Expr Patterns*. 2016;20:42-54.
15. Barbosa JS, Sanchez-Gonzalez R, Di Giaino R, et al. Neurodevelopment. Live imaging of adult neural stem cell behavior in the intact and injured zebrafish brain. *Science*. 2015;348:789-793.
16. Diotel N, Vaillant C, Gabbero C, et al. Effects of estradiol in adult neurogenesis and brain repair in zebrafish. *Horm Behav*. 2013;63:193-207.
17. Baumgart EV, Barbosa JS, Bally-Cuif L, et al. Stab wound injury of the zebrafish telencephalon: a model for comparative analysis of reactive gliosis. *Glia*. 2012;60:343-357.
18. Kishimoto N, Shimizu K, Sawamoto K. Neuronal regeneration in a zebrafish model of adult brain injury. *Dis Model Mech*. 2012;5:200-209.
19. Kroehne V, Freudenreich D, Hans S, Kaslin J, Brand M. Regeneration of the adult zebrafish brain from neurogenic radial glia-type progenitors. *Development*. 2011;138:4831-4841.
20. März M, Schmidt R, Rastegar S, Strähle U. Regenerative response following stab injury in the adult zebrafish telencephalon. *Dev Dyn*. 2011;240:2221-2231.
21. Schmidt R, Beil T, Strähle U, et al. Stab wound injury of the zebrafish adult telencephalon: a method to investigate vertebrate brain neurogenesis and regeneration. *J Vis Exp*. 2014;90:e51753.
22. Kyritsis N, Kizil C, Zocher S, et al. Acute inflammation initiates the regenerative response in the adult zebrafish brain. *Science*. 2012;338:1353-1356.
23. Diotel N, Beil T, Strähle U, Rastegar S. Differential expression of id genes and their potential regulator znf238 in zebrafish adult neural progenitor cells and neurons suggests distinct functions in adult neurogenesis. *Gene Expr Patterns*. 2015;19:1-13.
24. Diotel N, Rodriguez Viales R, Armant O, et al. Comprehensive expression map of transcription regulators in the adult zebrafish telencephalon reveals distinct neurogenic niches. *J Comp Neurol*. 2015;523:1202-1221.
25. Rodriguez Viales R, Diotel N, Ferg M, et al. The helix-loop-helix protein id1 controls stem cell proliferation during regenerative neurogenesis in the adult zebrafish telencephalon. *STEM CELLS*. 2015;33:892-903.
26. Aleström P, D'Angelo L, Midtlyng PJ, et al. Zebrafish: housing and husbandry recommendations. *Lab Anim*. 2019;23677219869037. <https://doi.org/10.1177/0023677219869037>.
27. Engstrom PG, Fredman D, Lenhard B. Ancora: a web resource for exploring highly conserved noncoding elements and their association with developmental regulatory genes. *Genome Biol*. 2008;9:R34.
28. Navratilova P, Fredman D, Hawkins TA, Turner K, Lenhard B, Becker TS. Systematic human/zebrafish comparative identification of cis-regulatory activity around vertebrate developmental transcription factor genes. *Dev Biol*. 2009;327:526-540.
29. Ishibashi M, Mechaly AS, Becker TS, Rinkwitz S. Using zebrafish transgenesis to test human genomic sequences for specific enhancer activity. *Methods*. 2013;62:216-225.
30. Schindelin J, Arganda-Carreras I, Frise E, et al. Fiji: an open-source platform for biological-image analysis. *Nat Methods*. 2012;9:676-682.
31. Armant O, März M, Schmidt R, et al. Genome-wide, whole mount in situ analysis of transcriptional regulators in zebrafish embryos. *Dev Biol*. 2013;380:351-362.
32. Meng A, Tang H, Ong BA, Farrell MJ, Lin S. Promoter analysis in living zebrafish embryos identifies a cis-acting motif required for neuronal expression of GATA-2. *Proc Natl Acad Sci U S A*. 1997;94:6267-6272.
33. Cartharius K, Frech K, Grote K, et al. MatInspector and beyond: promoter analysis based on transcription factor binding sites. *Bioinformatics*. 2005;21:2933-2942.
34. Korchynskiy O, ten Dijke P. Identification and functional characterization of distinct critically important bone morphogenetic protein-specific response elements in the Id1 promoter. *J Biol Chem*. 2002;277:4883-4891.
35. Lopez-Rovira T, Chaux E, Massague J, et al. Direct binding of Smad1 and Smad4 to two distinct motifs mediates bone morphogenetic protein-specific transcriptional activation of Id1 gene. *J Biol Chem*. 2002;277:3176-3185.
36. Lewis TC, Prywes R. Serum regulation of Id1 expression by a BMP pathway and BMP responsive element. *Biochim Biophys Acta*. 1829;2013:1147-1159.

37. Hollnagel A, Oehlmann V, Heymer J, Rütther U, Nordheim A. Id genes are direct targets of bone morphogenetic protein induction in embryonic stem cells. *J Biol Chem*. 1999;274:19838-19845.
38. Henningfeld KA, Rastegar S, Adler G, Knöchel W. Smad1 and Smad4 are components of the bone morphogenetic protein-4 (BMP-4)-induced transcription complex of the Xvent-2B promoter. *J Biol Chem*. 2000;275:21827-21835.
39. Coltery RF, Link BA. Dynamic smad-mediated BMP signaling revealed through transgenic zebrafish. *Dev Dyn*. 2011;240:712-722.
40. Laux DW, Febbo JA, Roman BL. Dynamic analysis of BMP-responsive smad activity in live zebrafish embryos. *Dev Dyn*. 2011;240:682-694.
41. Schiavone M, Rampazzo E, Casari A, et al. Zebrafish reporter lines reveal in vivo signaling pathway activities involved in pancreatic cancer. *Dis Model Mech*. 2014;7:883-894.
42. Hao J, Ho JN, Lewis JA, et al. In vivo structure-activity relationship study of dorsomorphin analogues identifies selective VEGF and BMP inhibitors. *ACS Chem Biol*. 2010;5:245-253.
43. Hao J, Lee R, Chang A, et al. DMH1, a small molecule inhibitor of BMP type I receptors, suppresses growth and invasion of lung cancer. *PLoS One*. 2014;9:e90748.
44. Kizil C, Kyritsis N, Brand M. Effects of inflammation on stem cells: together they strive? *EMBO Rep*. 2015;16:416-426.
45. Alunni A, Krecsmarik M, Bosco A, et al. Notch3 signaling gates cell cycle entry and limits neural stem cell amplification in the adult pallium. *Development*. 2013;140:3335-3347.
46. Than-Trong E, Ortica-Gatti S, Mella S, Nepal C, Alunni A, Bally-Cuif L. Neural stem cell quiescence and stemness are molecularly distinct outputs of the Notch3 signalling cascade in the vertebrate adult brain. *Development*. 2018;145:dev161034.
47. Bond AM, Peng CY, Meyers EA, McGuire T, Ewaleifoh O, Kessler JA. BMP signaling regulates the tempo of adult hippocampal progenitor maturation at multiple stages of the lineage. *STEM CELLS*. 2014;32:2201-2214.
48. Mira H, Andreu Z, Suh H, et al. Signaling through BMPRII regulates quiescence and long-term activity of neural stem cells in the adult hippocampus. *Cell Stem Cell*. 2010;7:78-89.
49. Nam HS, Benezra R. High levels of Id1 expression define B1 type adult neural stem cells. *Cell Stem Cell*. 2009;5:515-526.
50. Imayoshi I, Sakamoto M, Yamaguchi M, Mori K, Kageyama R. Essential roles of notch signaling in maintenance of neural stem cells in developing and adult brains. *J Neurosci*. 2010;30:3489-3498.
51. Blomfield I, Rocamonde B, Masdeu M, et al. Id4 eliminates the pro-activation factor Ascl1 to maintain quiescence of adult hippocampal stem cells. *bioRxiv*. 2018.
52. Boareto M, Iber D, Taylor V. Differential interactions between notch and ID factors control neurogenesis by modulating Hes factor autoregulation. *Development*. 2017;144:3465-3474.
53. Rastegar S, Hess I, Dickmeis T, et al. The words of the regulatory code are arranged in a variable manner in highly conserved enhancers. *Dev Biol*. 2008;318:366-377.
54. Kusanagi K, Inoue H, Ishidou Y, Mishima HK, Kawabata M, Miyazono K. Characterization of a bone morphogenetic protein-responsive Smad-binding element. *Mol Biol Cell*. 2000;11:555-565.
55. Yoshida Y, Tanaka S, Umemori H, et al. Negative regulation of BMP/Smad signaling by Tob in osteoblasts. *Cell*. 2000;103:1085-1097.
56. Dennler S, Itoh S, Vivien D, ten Dijke P, Huet S, Gauthier JM. Direct binding of Smad3 and Smad4 to critical TGF beta-inducible elements in the promoter of human plasminogen activator inhibitor-type 1 gene. *EMBO J*. 1998;17:3091-3100.
57. Zawel L, Dai JL, Buckhaults P, et al. Human Smad3 and Smad4 are sequence-specific transcription activators. *Mol Cell*. 1998;1:611-617.
58. Monteiro RM, de Sousa Lopes SM, Bialecka M, et al. Real time monitoring of BMP Smads transcriptional activity during mouse development. *Genesis*. 2008;46:335-346.
59. Ramel MC, Hill CS. The ventral to dorsal BMP activity gradient in the early zebrafish embryo is determined by graded expression of BMP ligands. *Dev Biol*. 2013;378:170-182.
60. Ionescu AM, Drissi H, Schwarz EM, et al. CREB cooperates with BMP-stimulated Smad signaling to enhance transcription of the Smad6 promoter. *J Cell Physiol*. 2004;198:428-440.
61. Ohta Y, Nakagawa K, Imai Y, Katagiri T, Koike T, Takaoka K. Cyclic AMP enhances Smad-mediated BMP signaling through PKA-CREB pathway. *J Bone Miner Metab*. 2008;26:478-484.

#### SUPPORTING INFORMATION

Additional supporting information may be found online in the Supporting Information section at the end of this article.

**How to cite this article:** Zhang G, Ferg M, Lübke L, et al. Bone morphogenetic protein signaling regulates Id1-mediated neural stem cell quiescence in the adult zebrafish brain via a phylogenetically conserved enhancer module. *Stem Cells*. 2020;38:875-889. <https://doi.org/10.1002/stem.3182>